

MICROCOPY RESOLUTION TEST CHART

NATIONAL BUREAU OF STANDARDS-1963-A

AFOSR-TR- 80 - 0137

12
R

LEVEL II

ADA 081 476

TRIBOSTIMULATED EXOEMISSION FROM OXIDE COVERED METALS

J. T. Dickinson and P. F. Braunlich
Physics Department
Washington State University
Pullman, WA 99164

January 1980

Final Report for Period June 1978 - October 1979

Grant No. AFOSR 78-3650

Approved for public release; distribution unlimited

Prepared for: Air Force Office of Scientific Research

S MAR 6 1980 A

FILE COPY

80 3 3 022

UNCLASSIFIED

SECURITY CLASSIFICATION OF THIS PAGE (When Data Entered)

REPORT DOCUMENTATION PAGE		READ INSTRUCTIONS BEFORE COMPLETING FORM	
1. REPORT NUMBER AFOSR-TR-80-0137	2. GOVT ACCESSION NO.	3. RECIPIENT'S CATALOG NUMBER 9 1	
4. TITLE (and Subtitle) TRIBOSTIMULATED EXOEMISSION FROM OXIDE COVERED METALS.		5. TYPE OF REPORT & PERIOD COVERED Final Report, 1 June 78 - 31 October 79	
6. PERFORMING ORG. REPORT NUMBER		7. CONTRACT OR GRANT NUMBER(s) AFOSR-78-3650	
8. AUTHOR J. T. Dickinson and P. F. Bräunlich		9. PERFORMING ORGANIZATION NAME AND ADDRESS Physics Department Washington State University Pullman, WA 99164	
10. PROGRAM ELEMENT, PROJECT, TASK AREA & WORK UNIT NUMBERS 2306/421 6702F		11. CONTROLLING OFFICE NAME AND ADDRESS Air Force Office of Scientific Research Building 410 Bolling Air Force Base, Washington, D.C. 20332	
12. REPORT DATE January 1980		13. NUMBER OF PAGES 55	
14. MONITORING AGENCY NAME & ADDRESS (if different from Controlling Office)		15. SECURITY CLASS. (of this report) Unclassified	
15a. DECLASSIFICATION/DOWNGRADING SCHEDULE		16. DISTRIBUTION STATEMENT (of this Report) Approved for Public Release; distribution unlimited.	
17. DISTRIBUTION STATEMENT (of the abstract entered in Block 20, if different from Report)			
18. SUPPLEMENTARY NOTES			
19. KEY WORDS (Continue on reverse side if necessary and identify by block number) Adhesive Bonding Exoemission Chemiluminescence Anodic Films Particle Emission Aluminum Anodizing Acoustic Emission Oxide Coatings Brittle Fracture			
20. ABSTRACT (Continue on reverse side if necessary and identify by block number) This report presents a summary of the work performed by Washington State University under Grant No. 78-3650 during June 1978 to October 1979. This report covers a number of experiments concerning emission phenomena accompanying plastic deformation of anodized aluminum. The sensitivity of this tribostimulated exoemission to anodization parameters and the relation of this emission to oxide cracking is briefly discussed. The emission of neutral species during deformation is presented. The comparison of acoustic emission			

DD FORM 1473 1 JAN 73

Unclassified

SECURITY CLASSIFICATION OF THIS PAGE (When Data Entered)

40-1959

113

#20. Abstract (continued)

Due to cracking of the anodized oxide layer with the accompanying electron emission shows the intimate link between fracture of the oxide layer and electron emission. We have also studied a model exoemission system (NaCl) to examine the details of the emission mechanisms of neutral species and electrons following perturbations due to electron bombardment. Finally we examine briefly the chemiluminescence that occurs during H_3PO_4 anodization of Al.

A

A

FOREWORD

This final report was prepared by Washington State University, Pullman, Washington under Grant AFOSR 78-3650. The work was administered under the direction of Major W. C. Simmons, Electronic and Solid State Services, AFOSR.

The personnel who have contributed to this research are: J. T. Dickinson, P. F. Bräunlich, E. E. Donaldson, L. A. Larson, D. L. Doering, and D. B. Snyder.

Technical Administration Officer

SUMMARY

This report discusses work performed at Washington State University from June 1978 to October 1979. The principle objective was to explore further the emission of particles from anodized aluminum during tensile deformation. Our major goals have been first to provide experimental evidence of the use of this emission to characterize anodized oxide films and second, to provide insight into the mechanisms for this emission. In this period we have concentrated on (a) the neutral emission component from anodized aluminum and (b) the correlation of electron emission with the acoustic emission from oxide layer cracking. As a means of testing proposed mechanisms for neutral and electron emission we have also examined (c) the emission of Cl atoms, Na atoms, and electrons from a more idealized material, NaCl after electron bombardment. We also report on some preliminary results on another emission system, namely photon emission during H_3PO_4 anodization.

A summary of the results are as follows:

- (a) An intense component of neutral emission clearly accompanies fracture of the oxide coating during deformation. The evidence we present indicates oxide cracking is necessary for the release of neutral molecules, there is a time decay of tenths of seconds suggesting a diffusion process, and the gaseous species observed are most likely due to trapped impurities within the oxide structure. There is also clear evidence of a thermal activation step, where the motion of the crack tip through the oxide is the likely source of heat.

- (b) Comparison of Acoustic Emission (AE) due to cracking of the anodized oxide layer with the accompanying electron emission (EE) shows that the electron emission is intimately related to crack propagation in the oxide. The AE and EE count rates vs. strain are closely related, most electron bursts are in near coincidence with an AE burst (therefore crack propagation), and most EE occurs within a few microseconds of crack propagation. There appears to be two components of EE: one occurring at crack-tip propagation and the other following propagation with a decay time of a few microseconds. We also have evidence of a component of EE unrelated to EE which is attributed to chemi-emission.
- (c) As a means of clarifying some of the mechanisms of neutral atom and electron emission we investigated a model system, namely thermal stimulated emission from electron bombarded NaCl. Here the primary defects produced are much better understood and the processes that occur during heating could be better established. We provide direct evidence of atomic Cl emission via V_k -Center decomposition, the emission of exoelectrons due to a chemi-emissive process, and thermal desorption of Cl. Analogous processes are believed to be occurring in tribo-stimulated exoemission.
- (d) We have found that during H_3PO_4 anodization of Bare Al 2024 and Al 1350 easily observable photon emission is detected. Preliminary results show that this emission occurs at very low anodization potentials which suggests a form of chemiluminescence during oxidation. Such emission could be very useful for monitoring the anodization used for preparing Al for epoxy bonding.

TABLE OF CONTENTS

	Page
FOREWARD.	1
SUMMARY	11
SECTION	
I. INTRODUCTION	1
II. CHARACTERIZATION OF ANODIZED OXIDE FILMS BY EXOEMISSION AND ACOUSTIC EMISSION	2
A. Introduction	2
B. Procedure and Comments	2
C. Results	4
D. Conclusions	10
III. THE EMISSION OF NEUTRAL PARTICLES FROM ANODIZED ALUMINUM SURFACES DURING TENSILE DEFORMATION	11
A. Introduction	11
B. Experimental	12
C. Results	12
D. Discussion	20
IV. ACOUSTIC EMISSION AND ELECTRON EMISSION DURING DEFORMATION OF ANODIZED ALUMINUM	23
A. Introduction	23
B. Experiment	23
C. Results	25
D. Discussion	33
V. EMISSION OF Cl ATOMS FROM NaCl DURING V_k -CENTER DECOMPOSITION	35
A. Introduction	35
B. Experimental Procedure	37
C. Results	38
D. Conclusions	42
VI. CHEMILUMINESCENCE DURING H_3PO_4 ANODIZATION OF BARE Al 2024	43
VII. PUBLICATIONS AND PRESENTATIONS	45
VIII. REFERENCES	47

I. INTRODUCTION

Exoelectron emission is generally due to the release of highly localized energy at the surface of a solid in a relatively short time period. Many competing processes can dissipate this energy, particle emission being one of the least likely and phonon production being the most likely. The emission we observe in these experiments can be directly correlated with the propagation of cracks in the oxide coating. The manner in which an oxide coating responds to uniform straining of the aluminum substrate and the resulting emission of particles is strongly dependent on the mechanical and chemical nature of the oxide coating. These physical and mechanical properties can play an important role in the adhesive bonding characteristics and/or corrosion resistance of the films--extremely important roles in applications. An overall test of an oxide layer sensitive to a number of oxide properties is difficult to find. It has been with this thought in mind that we first began examining tribo-stimulated exoemission from anodized oxide films.

In this report we first summarize recent data on a series of samples prepared by the Boeing Co. and give our conclusions concerning the use of exoemission as a means of detecting differences in oxide layers. We then examine neutral emission in comparison to electron emission. We discuss the correlation between acoustic emission and electron emission. We also present work on a model exoemission system NaCl which clarifies some of the mechanisms which might be active in tribostimulated exoemission. Finally we examine briefly another emission phenomenon, the chemiluminescence that occurs during anodization of Al in H_3PO_4 .

II. CHARACTERIZATION OF ANODIZED OXIDE FILMS BY EXOEMISSION AND ACOUSTIC EMISSION

A. Introduction

As already reported¹⁻³ we have examined the electron emission (EE) from anodized oxide layers on a number of substrates. Recently we have added the detection of acoustic emission (AE) from such samples. As will be shown in Part III, the majority of AE observed from soft aluminum substrates is from oxide cracking and the EE correlates strongly with this AE.

On alloy substrates there is a larger component of AE from the substrate itself. Also, the Boeing "Baseline" oxide on both bare and clad Al 2024 does not seem to crack very much during plastic deformation of the aluminum. This fact is determined by optical microscopy of the samples during elongation. The cracks are very sparsely distributed and tend to be relatively short, with no particular orientation relative to the strain axis. This leads to somewhat weak EE and AE due to oxide cracking.

B. Procedure and Comments

The sample sets provided for this study were anodized by the Boeing Co. according to Boeing Baseline specifications (a H_3PO_4 anodization) except the temperature of the anodization bath was varied. The temperatures were: 62°, 72° (Baseline), and 82° for both Al 2024 bare and clad. We found detectable EE for each set of samples provided and we also found a substantial change in the AE observed as we changed from one set of samples to another.

These particular samples differed from supposedly identical samples produced previously at Boeing¹ and our laboratory² in the following ways:

- (a) The total electron emission from the deformed samples was smaller by a factor of 10 on Al 2024 bare.
- (b) The cracks on the bare samples were not as long and numerous as on earlier samples, in agreement with (a).
- (c) The variation over a set of samples was greater for these samples than in the past.
- (d) The dependence of total EE on anodization temperature for Al 2024 clad came out different from an "equivalent" series anodized in our laboratory.²

These differences may well be due to small procedural changes or perhaps treatment after anodization. We tried to keep our handling of the samples as rigidly controlled as possible. For future comparison we outline this procedure as follows:

Following receipt of the samples from Boeing we stored them in a desiccator to keep them free of excess moisture. Just before mounting in the vacuum system, the sample was rinsed thoroughly in clean acetone. The sample was placed in the straining apparatus (see Ref. 3) and an acoustic emission transducer was attached near one end of the sample. The system was pumped down to 2×10^{-6} Torr, then strained uniaxially to 18% strain. The electron detector is a channeltron electron multiplier positioned 1 cm away from the sample and biased +300V relative to the ground sample.

The electronic discriminators, amplifiers, count-rate meters, and chart recorders were all maintained at constant levels for each run. We are confident that the major source of variation between samples within a set (as well as between sets of "identical" samples) is primarily changes in the oxides. When samples are produced and handled identically in our laboratory

we find agreement in the basic features and total EE to within 8% deviation. Identical samples have the same crack densities after straining and should have close to identical physical and chemical structure. Since these are the factors that determine the EE behavior, we conclude that significant differences (8%) in the observed EE are due to differences in the oxide. This could be due to a number of factors which include the following:

1. Differences in the Anodization Procedure (see Ref. 2) either before, during, or directly after anodization.
2. Contamination of the Anodization Bath.
3. Differences in the Surface of the Oxide, e.g. contamination or damage due to handling.
4. An Aging effect (see Ref. 2).

With the exception of No. 2, we have shown that the others can strongly influence the EE. We would suspect that contaminants in the anodization bath could also alter the EE through chemical alteration of the anodic film.

C. Results

In spite of the slight inconsistencies in comparison with previous results, we can nevertheless compare the six sets of samples provided and point out the substantial changes that occur between them.

To present the data, we first tabulate the total EE and AE for each of these sample sets, then present typical count-rate curves for each set.

Table I presents the averages for each set. Each set contains 5 to 10 samples and the uncertainty represents one standard deviation.

All samples yielded detectable exoemission above the background count rate, although the baseline Al 2024 Bare sample emission rate was very low. Nevertheless, deviations from Baseline anodization is detectable in both clad and bare.

Table 1. Summary of EE and AE Results on Clad and Bare Al 2024.

	Anodization Temperature	EE	AE
Al 2024 Clad	62F	2220± 600	11,600± 4,000
	72F	520± 100	4,600± 3,000
	82F	220± 80	2,500± 1,000
	No Oxide	4 (Background Counts)	22,300± 2,000
Al 2024 Bare	62F	255± 10	25,000± 11,000
	72F	50± 10	12,400± 3,000
	82F	135± 20	12,700± 3,000
	No Oxide	4 (Background Counts)	20,700± 7,000

The acoustic emission from these samples is very interesting. With the exception of the 62°F Al 2024 Base samples, the AE is substantially reduced from the AE with unanodized samples.

Several investigators (see Ref. 4, 5, 6) have shown a completely different trend, namely an increase in AE with the presence of oxide. In fact Dunegan and Tatro⁶ report that for Al 6061, the total number of AE bursts goes up with the fifth power of the oxide thickness (they do not specify their type of oxide). In our earlier work,¹ we showed that exoemission on clad and bare Al 2024 was also strongly dependent on oxide thickness. Part III of this report will show that one of the important parameters of the anodized oxide layer on Al 1350 that determines both the AE and EE totals is the number of crack increments that occur during straining.

To make all these results consistent we believe that in the case of Al 6061, they were observing AE from oxide cracking. In the case of our porous oxides on Al 2024, we feel that the oxide is inhibiting AE from the Al 2024 substrate. A possible cause of this reduction in AE due to the presence of the oxide is the prevention of slip step formation at the substrate surface. The latter is frequently associated with AE production in aluminum.

Thus it appears that for the porous oxides provided, very little AE is detected due to oxide cracking. However, the cracking that does occur leads to electron emission. Both the AE and EE show changes with the anodization bath temperature. The two types of emission used together might provide an even stronger indicator of the oxide coating.

Figure 1 presents typical data (count rate vs. strain) for the electron emission from Al 2024 clad samples anodized at the three different temperatures. The major difference seen are of course the shapes and intensities of the emission. The basic shapes were quite reproducible. The periodic structure which occurs at all temperatures but is most evident in the 72°F curves is due to an effect which is observed on Al 2024 but not on anodized pure Al or the purer alloys. It is a consequence of localized straining along the length of the gauge. The electron detector only views about 1 cm of the sample (determined by decreasing the length of the anodization region). If the sample ceases to elongate for a short time within this 1 cm interval the oxide cracking would cease and the accompanying emission would also cease. When the surface of a sample is viewed under a microscope during uniform elongation one can easily see that locally the strain starts and stops somewhat periodically. A student, Dave Snyder, is currently examining mechanisms of plastic deformation in aluminum alloys to explain this effect. A simple way to avoid this "fine structure" would be to use an electron multiplier with a larger anode (e.g. a

Al 2024 Clad
H₃PO₄ Anodized

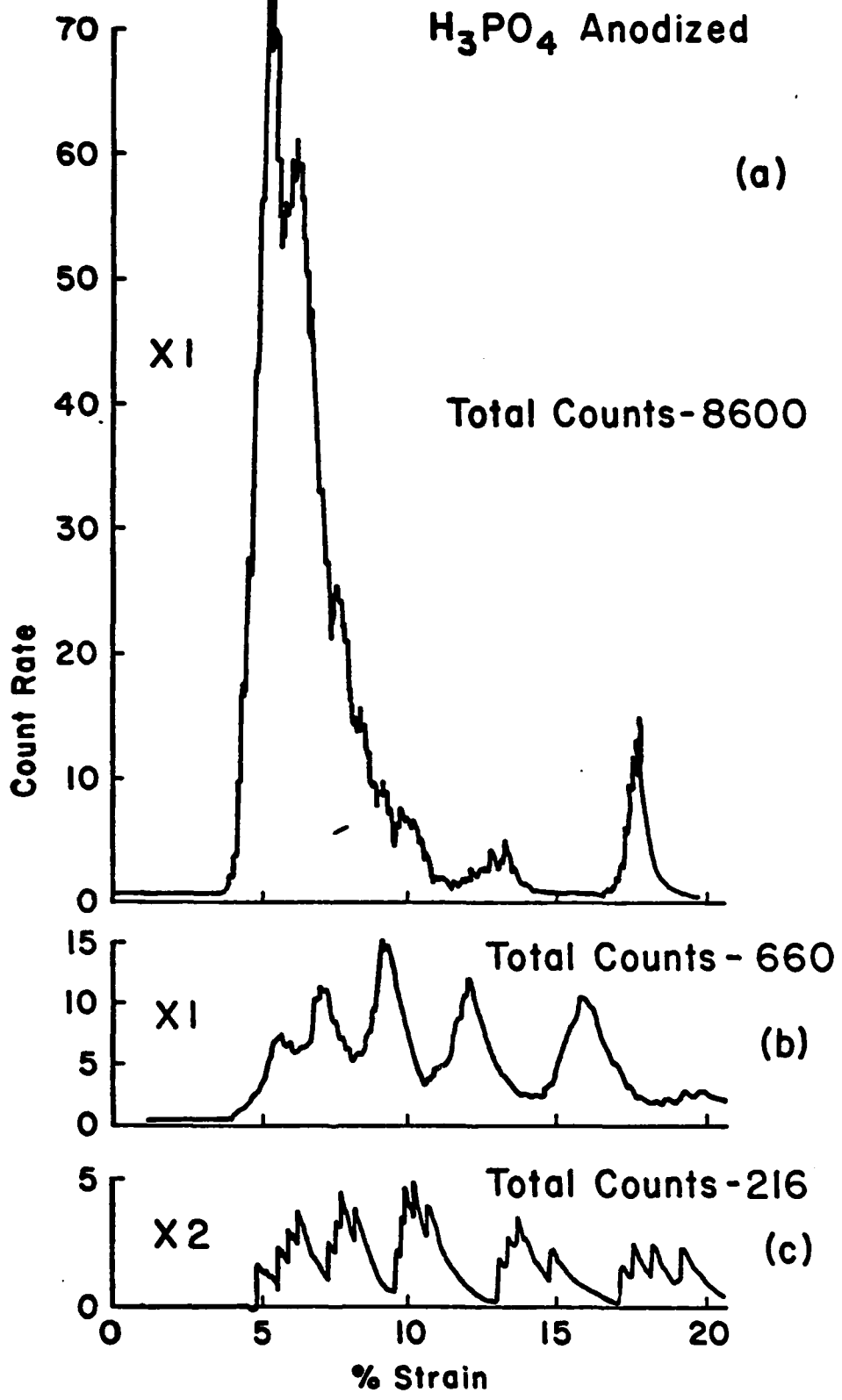


Fig. 1. Typical electron emission curves (count rate vs. strain) for three different anodization bath temperatures: anodized at (a) 62F, (b) 72F, (c) 82F.

channeltron with a cone) and stronger electric fields to increase the collection efficiency from the entire length of the sample.

Figure 2 is a similar set of data for Al 2024 Bare. Although the emission is quite weak it is well above background (the number of counts due to background is 2-5 counts for the duration of the test). We also see that the basic shape of the emission curve is different from the clad samples, namely a rise in emission intensity as the sample elongates. This basic shape is in good agreement with our previous work.^{1,2} Finally we note that the intensity indeed depends on anodization bath temperature.

Al 2024 Bare H_3PO_4 Anodized

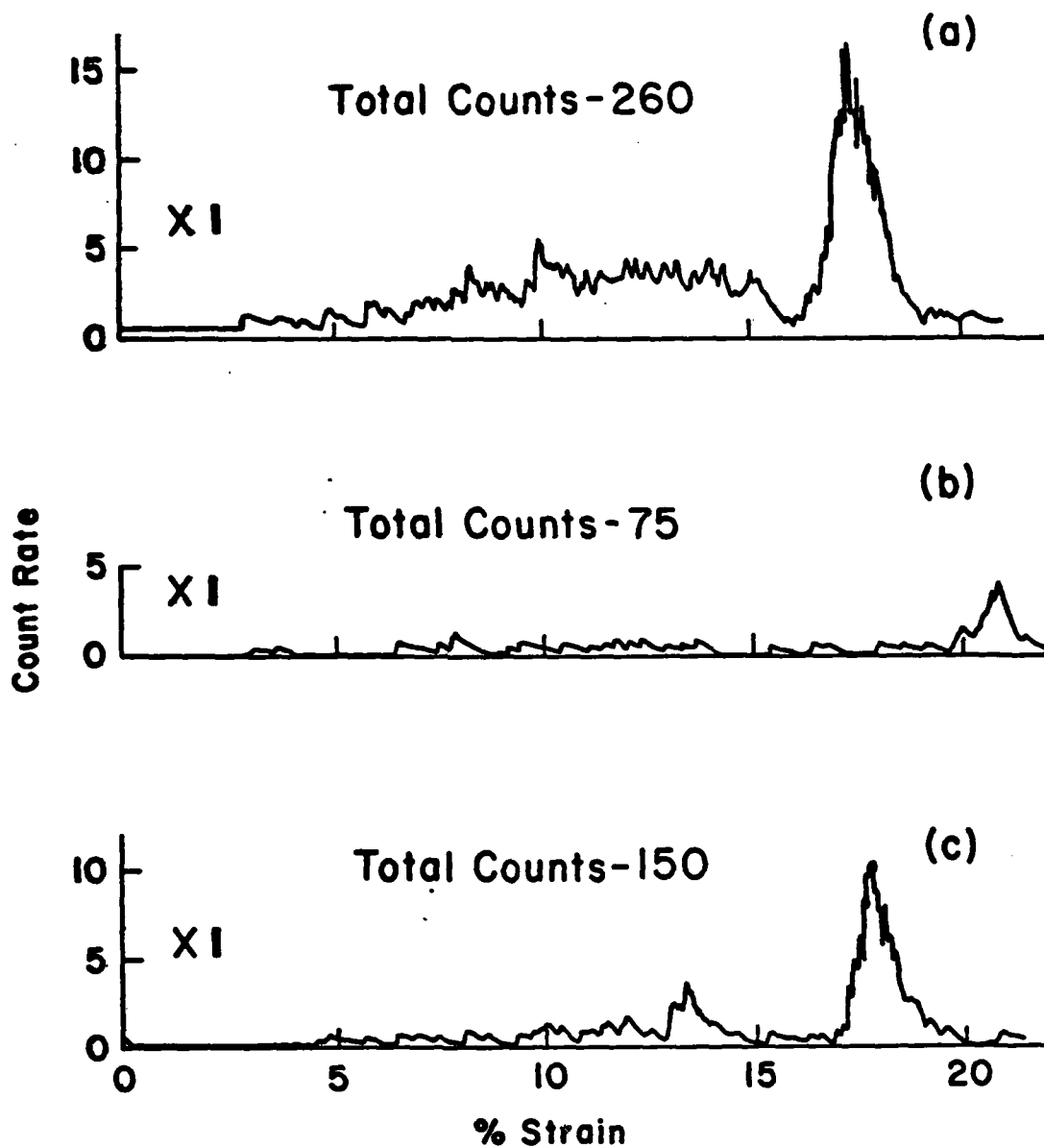


Fig. 2. Typical electron emission curves (count rate vs. strain) for Al 2024 Bare and three different anodization bath temperatures: anodized at (a) 62F, (b) 72F, (c) 82F.

D. Conclusions

As we have shown in the past (e.g. ref. 1,2) as well as here, tribo-stimulated exoemission is a sensitive probe of the physical and chemical properties of an anodized oxide coating. The results we have obtained here and earlier are consistent with optical and scanning electron microscopy and the hypothesis that oxide disruption (e.g. cracking) is a prerequisite for emission. The oxides studied here differ in their pore structure and their thickness, both of which can greatly influence the manner in which the films respond to tensile deformation. A simple example is when the oxide becomes thick and the pores more columnar, we observe an increased exoemission.² Similarly for a given thickness, as the oxide becomes more porous and "fluffy," the exoemission decreases.² Both of these results are due to the fact that the nature and number of cracks in the oxide are strongly dependent on these oxide characteristics.

Although the AE results also show sensitivity to the oxide on 2024 Al clad, it appears to be such that the oxide tends to inhibit AE. This is somewhat more difficult to use as a probe of oxide character. Nevertheless in conjunction with EE, the AE might be very useful in providing unambiguous characterization of oxide films. In section III, we shall explore the correlation of AE and EE where almost all of the AE is coming from oxide cracking.

III. THE EMISSION OF NEUTRAL PARTICLES FROM ANODIZED ALUMINUM SURFACES DURING TENSILE DEFORMATION

A. Introduction

We have studied, for the first time, the emission of neutral particles from anodic oxide coatings during the mechanical deformation of a material. This work is in conjunction with an effort to characterize anodic oxide layers through the effect of tribostimulated exoemission.^{1,3} Tribostimulated exoemission refers to the emission of electrons, ions, photons, and neutral particles during mechanical deformation. We have shown that electron exoemission is a very sensitive test of oxide thickness and structure, and thus is particularly suitable for applications where quality control of anodic oxide layers is important.^{1,3}

In this work we study the emission of neutral particles from a few of the possible oxide-metal substrate systems. We report here the composition of the emitted gases, the dependence of neutral emission on oxide thickness, a comparison of the rate of neutral emission with the rate of crack growth in the oxide layer, and a model to explain the observed data. Furthermore, we suggest that neutral emission provides new information, complementary to electron exoemission, concerning the properties of the oxide.

B. Experimental

These experiments were performed in an UHV system, with a base pressure less than 10^{-7} Pa, which has been described previously.⁷ The equipment includes a fully instrumented tensile straining device, a quadrupole mass spectrometer for partial pressure analysis, and a Bayard-Alpert gauge to record total pressure. The experimental procedure involves deforming the anodized aluminum sample at a constant strain rate while simultaneously recording the partial pressure increase of the main emission products, the total pressure increase, and the stress-strain relationship. This allows correlation between emission of neutral particles and previously obtained electron emission curves.

A second UHV system was employed to perform thermal flash desorption experiments on similarly prepared anodized aluminum samples. This system has also been previously described.⁸ In addition, optical microscopy and a high resolution SEM were used to characterize the oxide layers and the relationship between crack density and strain.

Standard anodization procedures¹ were used to produce the oxide coatings on both bare and clad 2024 Al. Dense barrier type oxides were prepared using an ammonium tartrate electrolyte. Porous duplex oxides were prepared using a phosphoric acid electrolyte. In some cases, oxide thickness was purposefully varied. All of the data reported, with this exception, were run at a constant nominal 3000 Å oxide thickness.

C. Results

A typical neutral emission versus strain curve for a bare 2024 Al sample, anodized in ammonium tartrate, is shown in Fig. 3. These curves are characterized by a relatively steep initial rise in pressure followed by a

Neutral Emission v.s. Strain
Dense Oxide 3000 Å on Bare 2024

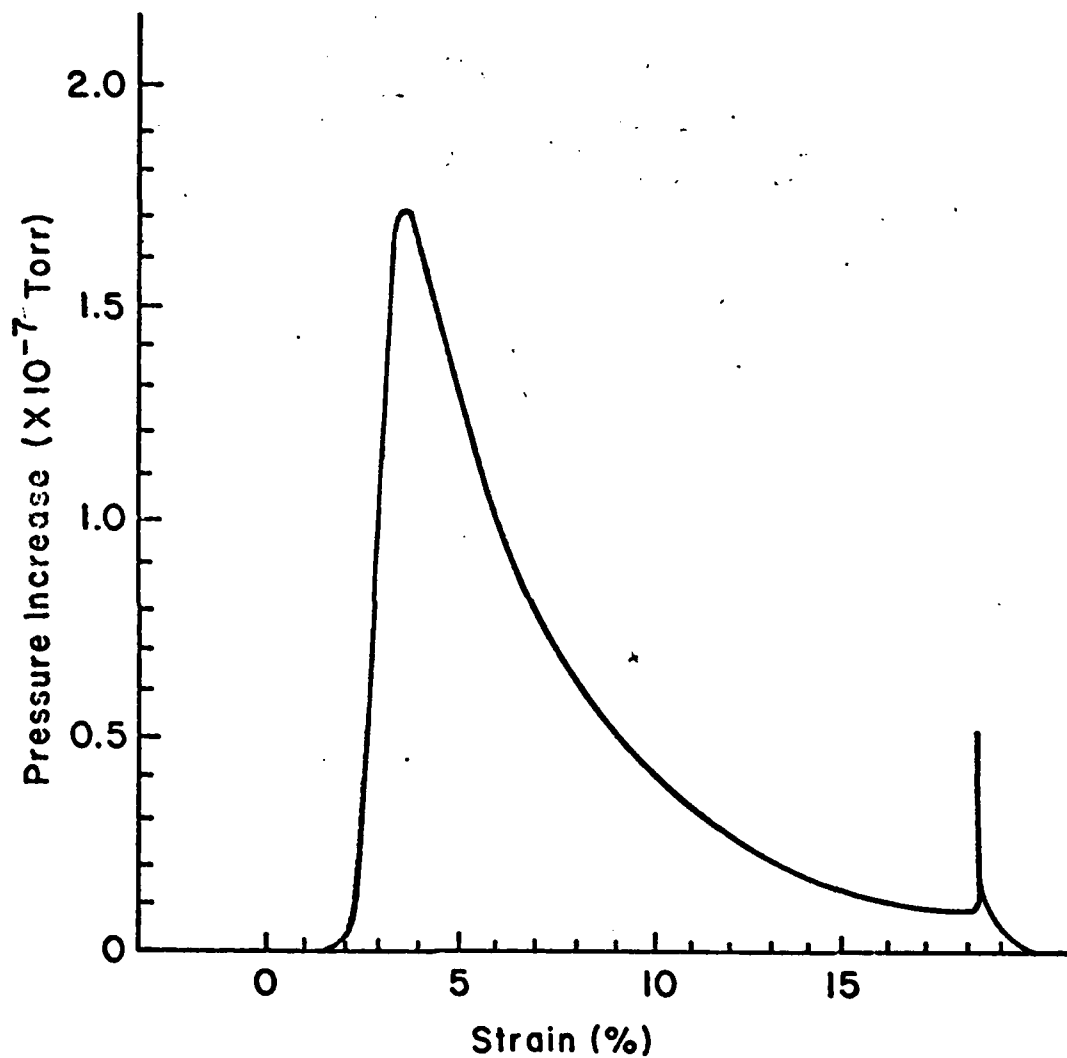


Fig. 3. A typical neutral emission versus strain curve for a 3000 Å dense oxide on bare Al 2024, produced at a strain rate of 0.084%/second.

slow decrease. The curve ends with a sudden burst of pressure which correlates with the rupture of the sample. Control experiments performed on unanodized samples indicate that the observed emission is due solely to the presence of the aluminum oxide layer. In addition, as will be seen later, the anodization electrolyte and the type of metal substrate (e.g. clad versus bare) are factors which effect the observed neutral emission.

Table 2 presents parameters of interest for neutral emission and exoelectron emission curves for a number of oxide-alloy systems. It is seen that both types of emission are more intense from dense oxides than from porous oxides. Although the peak positions for neutral emission and electron emission are virtually identical, the full-width of the curve at half maximum is considerably larger for neutral emission due to the long tail occurring after maximum neutral emission. Also, we note that the onset of emission is earlier for neutral emission than for electron emission.

An interesting observation is that the observed flux of neutral particles is a relatively intense effect. For a 3000 Å dense oxide on bare 2024 Al, the total emission of neutral particles is calculated to be 2×10^{17} molecules. This figure is approximately 15% of the total number of Al_2O_3 molecules which are expected to make up a 3000 Å layer. The emission from dense oxides on clad 2024 Al is calculated to be 4×10^{16} molecules which is about 3% of the calculated number of Al_2O_3 molecules. The emission from porous oxides is seen to be at least one order of magnitude smaller than emission from dense oxides.

The emitted species were identified with a quadrupole mass spectrometer. O_2 and CO_2 molecules were the observed neutral species emitted from dense oxides produced by ammonium tartrate anodization. Only O_2 molecules were observed from porous oxides produced by phosphoric acid anodization. No other emitted species were identified and could at most contribute 0.5% of

TABLE 2
 Characteristic Emission Parameters for a Nominal 3000 Å Oxide

Sample and Type of Emission		Peak Height	Start	F.W.H.M. in % Strain	Peak Position
Clad 2024 Al	Dense Oxide Neutral Emission	2.5×10^{-8} Torr	1.5%	4.6%	3.2%
	Dense Oxide Electron Emission	1100 cps	~2%	2.1%	3.1%
	Porous Oxide Neutral Emission	3.8×10^{-9} Torr	1.4%	~6%	4.4%
	Porous Oxide Electron Emission	500 cps	~2%	2.9%	4.3%
Bare 2024 Al	Dense Oxide Neutral Emission	1.7×10^{-7} Torr	1.8%	3.8%	3.5%
	Dense Oxide Electron Emission	50 cps	2.8%	2.6%	4.1%
	Porous Oxide Neutral Emission	4.0×10^{-9} Torr	2.2%	13.2%	9.5%
	Porous Oxide Electron Emission	~15 cps	~3.8%	~12%	~10%

the total emission. One exception should be noted: one dense oxide on a bare 2024 Al sample was observed to emit H_2O during the final seconds before sample rupture and continued for about 2 minutes after the sample had been broken. After-emission (emission following rupture) has been noted in exoelectron emission for some cases.¹ However, the effect is not reliably reproducible for either neutral or exoelectron emission.

The dependence of neutral emission on thickness is illustrated in Fig. 4, for the case of dense oxides on bare 2024 Al. This curve shows that the neutral emission saturates at about 2500 Å nominal thickness, in contrast to exoelectron emission, which continues to climb at an exponential rate with thickness.¹ It is also seen that the ratio of O_2 emission to total emission decreases with increasing oxide thickness in a roughly linear fashion, from 75% for 350 Å to about 50% for 3500 Å.

Since one would expect some form of heating to be involved in the release of gas from the oxide, we performed thermal desorption experiments on a bare 2024 Al sample coated with a 3000 Å thick dense oxide. A 1.5 cm² sample, anodized in the same manner as the neutral emission samples, was mounted so that it could be heated in a UHV system at a linear rate. The emission of neutral particles during heating is observed with a quadrupole mass spectrometer. The major products observed were again O_2 and CO_2 . The observed thermal desorption peaks were approximately 300 K wide, considerably wider than the 30-50 K FWHM typically seen in monolayer desorption, and were also three orders of magnitude more intense. This indicates that thermal emission involves a considerable portion of the bulk and results from thermally activated processes (e.g. decomposition and/or diffusion) other than simple desorption of molecules adsorbed on the surface.

Neutral Emission v.s. Thickness Dense Oxide on Bare 2024

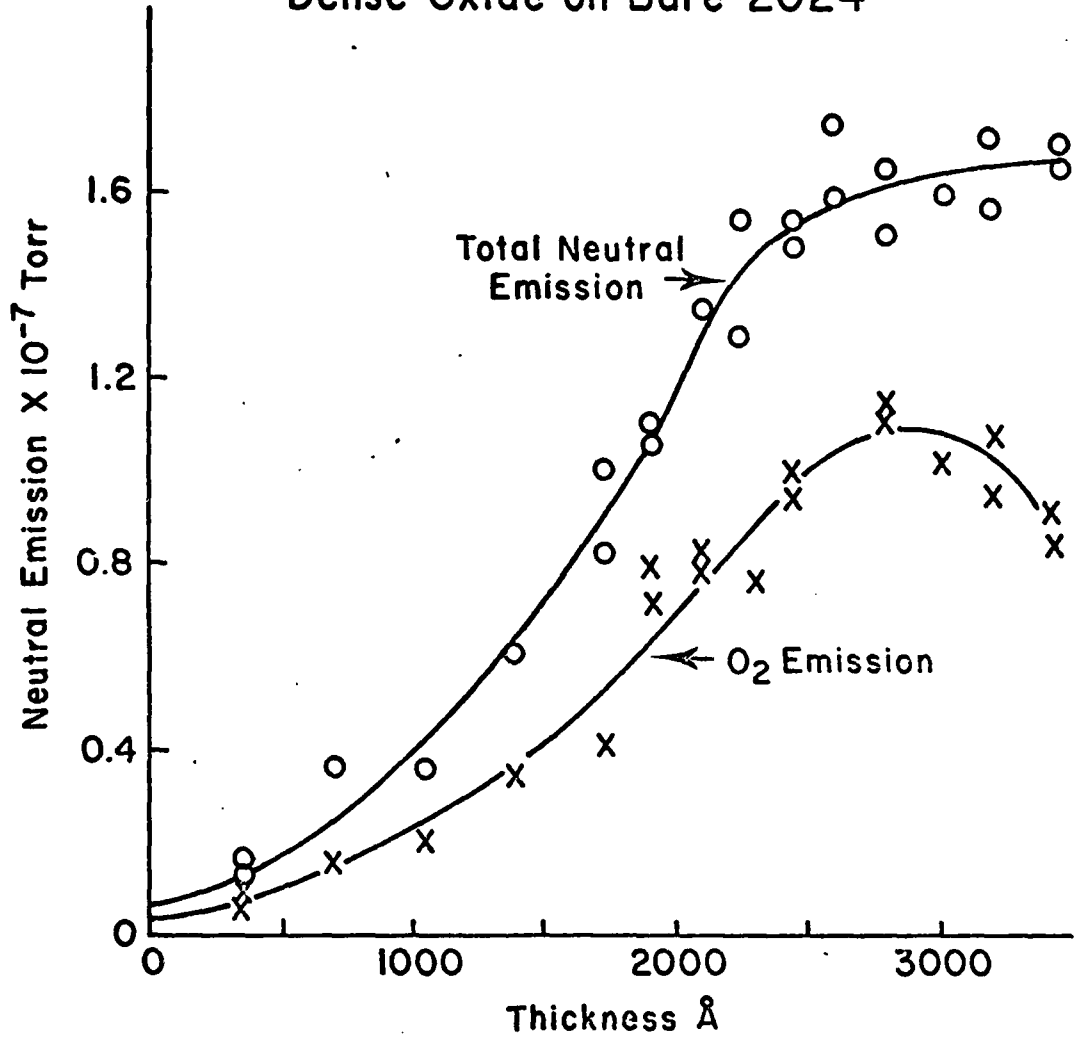


Fig. 4. Neutral emission intensity versus thickness for a dense oxide on bare Al 2024. xxx: peak heights of O₂ emission, ooo: peak heights of the total emission curves.

Interestingly, the form of the initial rise of the thermal emission for CO_2 was different from that of O_2 . This indicates that the rate limiting step of the mechanism of the thermal emission of these species is different. The initial rise of the CO_2 thermal emission has a functional dependence of $N \propto e^{-E/kT}$ with an activation energy of 7 kcal/mole (0.3 eV); while the initial rise of the O_2 thermal emission has a functional dependence of $N \propto e^{aT}$ where $a = 2 \times 10^{-2} \text{ K}^{-1}$.

In order to provide insight into the mechanisms responsible for both neutral emission and exoelectron emission, we compared these emission curves with measurements of the density of cracks as a function of strain, ϵ , in the aluminum oxides as observed with optical microscopy. Some models of exoelectron emission assume that the rate of emission is strictly proportional to the derivative of total crack length with strain,^{3,9} $dL/d\epsilon$, i.e., the rate of crack formation. Typical neutral emission and exoelectron emission curves are shown in Fig. 5, for a dense oxide on clad 2024 Al, along with the corresponding $dL/d\epsilon$ curve. Interestingly, neither the exoelectron emission nor the neutral emission curve is directly proportional to this derivative. Concentrating on the neutral emission, let us examine a simple model relating crack growth and neutral emission. We will assume that the emission occurs from freshly opened cracks and decays with time as e^{-bt} , suggestive of a diffusion limited process. For a sufficiently slow decay relative to the time constants for our electronics and vacuum system pumping speed, we may obtain the value of the constant b by stopping the pull and observing the decay of the emission with time. The decay was indeed observable and yielded decay constants of 0.10 sec^{-1} for O_2 and 0.17 sec^{-1} for CO_2 .

A calculated neutral emission curve was thus produced by assuming that the two types of molecules, O_2 and CO_2 , are released from cracks, created at

Dense Oxide on Clad 2024

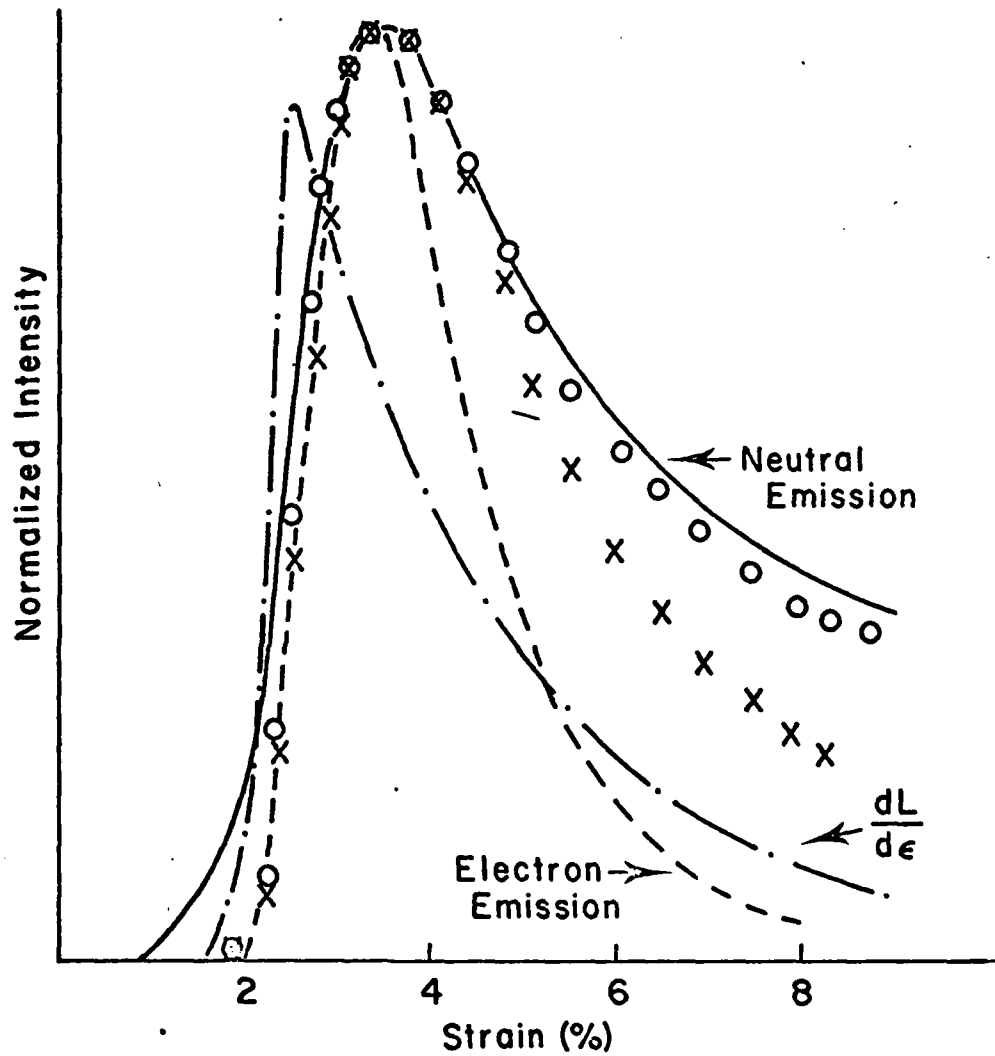


Fig. 5. Emission curves and the derivative of crack length with respect to strain for a dense oxide on clad Al 2024.
 xxx: calculated from the emission decay model,
 ooo: calculated from the emission decay model corrected for sample geometry and strain distribution.

a rate given by the curve for $dL/d\varepsilon$, and which then leaks out of the cracks with the above measured decay constants. The resulting expression for the rate of neutral emission is:

$$N(\varepsilon) = N_0 \int_0^\varepsilon \frac{dL(\varepsilon')}{d\varepsilon'} e^{-b(\varepsilon-\varepsilon')} d\varepsilon' \quad (3)$$

where $N(\varepsilon)$ = rate of neutral emission
 N_0 = normalization constant
 $L(\varepsilon)$ = total crack length
 ε = strain, where $\varepsilon = \alpha t$ (linear strain rate)

The emission curves for O_2 and CO_2 were then summed and renormalized. This is shown in Fig. 5 (represented by xxx). Note that this calculated curve falls off more rapidly for higher strains than the observed emission. We attribute this to the nonuniform strain at the ends of the sample which are normally left anodized. A simple correction to the $dL/d\varepsilon$ curve can be made for the contribution of the sample ends and yields a final calculated curve in Fig. 5 (represented by ooo), in fairly good agreement for most values of strain. To confirm the importance of this correction, we acid-etched the oxide from the ends of a sample before performing the neutral emission experiment and found that the emission curve generally agreed with the original calculated model (xxx) without the end correction.

The deviation of the observed neutral emission from the model curves at low strain is believed to be due to cracks that are too small to be observed with the optical microscope available.

D. Discussion

The structure of anodized aluminum oxides is known to be amorphous in nature with varying degrees of crystallinity depending upon the electrolyte and the anodizing conditions.⁹ It is also known that during the electrolytic

anodizing process, the anion is incorporated to some extent into the oxide¹¹⁻¹⁴ and that oxygen gas is evolved at the anode.¹⁰ We thus propose that the observed O_2 emission is due to the incorporation of oxygen atoms or molecules into the oxide film as impurities. Similarly, the CO_2 product in the dense ammonium tartrate oxides may be due to carboxyl groups of the tartrate anion which could be incorporated into the oxide structure either as a whole molecule or in a decomposed form. In any case, the sources of the neutral emission products are impurities trapped within the oxide structure.

We propose that the tribostimulated emission of neutral particles involves two critical steps:

- (1) Thermal activation: The shape of the thermal emission curves as well as similarities to the neutral emission, such as quantity of gas released and products observed, suggest that a thermal activation step occurs in tribo-stimulated neutral emission. This may involve desorption from impurity centers in the oxide or the decomposition of trapped anions. The necessary energy for this thermal activation could be supplied by the local heating which occurs during the propagation of the crack tip¹ through the oxide. This highly localized heating would be conducted away into the oxide, causing activation of the neutral emission sources in the vicinity of the newly formed crack. The time constant for the spread of this energy is expected to be on the order of microseconds or less.
- (2) Diffusion: The clear evidence for delays on the order of seconds in the release of the gas from the oxide indicates a diffusion process at room temperature. The conductance

of the newly formed cracks (and the pores in a porous oxide) is much too large to account for the observed decay constants. More likely, considering this long decay time, the diffusion paths involve imperfections in the oxide with dimensions on the order of the sizes of the diffusing molecules. The large quantity of gas emitted in both thermal emission and tribostimulated neutral emission indicate an extensive network of such diffusion paths, however at this point their nature is unknown.

In conclusion, the tribostimulated emission of neutral particles from anodically formed oxides has been shown to be intimately related to the propagation of cracks in the oxide. Equation (3) relating neutral emission with $dL/d\epsilon$ provides good agreement with the experimental emission provided an exponentially decaying release of gas from the sample is included. This decay suggests a diffusion step as part of the mechanism for neutral emission. It should be noted that for low strain rates, Eq. (3) approaches $N(\epsilon) \propto dL(\epsilon)/d\epsilon$, providing a direct measure of the crack length versus strain relationship.

Although the details of the mechanism for tribostimulated neutral emission need yet to be established, we suggest that the information obtained (e.g. shapes of the curves, identity and quantity of gaseous products released, and decay times) would be a useful technique for partial characterization of a number of nonductile coatings on ductile substrates.

IV. ACOUSTIC EMISSION AND ELECTRON EMISSION DURING DEFORMATION OF ANODIZED ALUMINUM

A. Introduction

Anodic oxide coatings are widely used in industry today. For example, two important uses of anodic oxide films on aluminum are as protective coatings and as preparation for epoxy bonding. There is considerable interest in characterizing oxide films and surfaces and in understanding the mechanical properties of oxide layers under stress.

We have been investigating the emission of different types of particles from anodized aluminum during uniaxial tensile deformation. The types of emission observed include electrons,⁽¹⁻³⁾ positive and negative ions,⁽¹⁾ photons,⁽¹⁾ and neutral molecules.⁽¹⁵⁾ The electron emission (EE) observed is often referred to as tribo-stimulated exo-electron emission because the deformation of the material leads to the emission. In general, the observed EE is closely associated with the production and growth of cracks in the oxide coating although the mechanism is not at all clear. In this paper, we present new experimental data relating EE and cracking of the oxide layer, leading to a better understanding of this phenomenon. An important new addition to our measurements is the detection of acoustic emission (AE) from the samples during their deformation in vacuum. We have evidence that the AE we observe actually accompanies the propagation of a crack in the oxide film. A major goal of this work has been to examine the correlation of EE and AE.

B. Experiment

The experimental details for observing tribostimulated exoemission from anodized aluminum samples may be found in references (1-3,15). The experiments we now describe were performed at a pressure of 10^{-4} Pa in a liquid nitrogen trapped diffusion-pumped vacuum system. This system could be recycled in 30 minutes

which allowed rapid data collection. The major features of the EE are unchanged when performed under UHV conditions (10^{-8} Pa).⁽²⁾ The electrons emitted during tensile deformation of the anodized samples were detected with a channeltron electron multiplier with an estimated quantum efficiency of 50-80%.⁽¹⁶⁾ The entrance to the electron multiplier was at a potential of +270 V relative to the sample (at ground) to enhance the collection efficiency.

The specimens were made from annealed Al 1350 sheet (99.5% pure) 1.14 mm in thickness, machined in a dogbone shape with a gage of 5 mm by 25 mm in dimension. The samples were cleaned in a $\text{CrO}_3\text{-H}_2\text{SO}_4$ solution and anodized in a 0.05 M ammonium tartrate solution at room temperature for 30 minutes at 230 V. This produces a very dense barrier type oxide with a thickness of 300 nm.⁽¹⁾ A commercial masking material was used to limit anodization to a small 30 mm^2 patch on one side near the center of the gage. The masking material was peeled off after anodization. When inserted into the pulling apparatus in the vacuum system, the oxide film faced the channeltron, approximately one centimeter away.

An acoustic transducer was attached to the center of the specimen on the side opposite the oxide film. The transducer was attached by a rubber band and a film of Apiezon N vacuum grease provided acoustic coupling to the specimen. Two AE transducers were used in this work: an AC 175 L and an AC 1500 L, both available from Acoustic Emission Technology Corporation. A broad-band pre-amplifier with 160 dB gain was used with appropriate filters to boost the signal-to-noise ratio. The signals associated with the AE during deformation were in the form of discontinuous bursts observed as ring down pulses. For the AC 175L the frequency of ringing was 170 kHz and typically 500 μs in duration. The AC 1500 L ringing occurred at 2 MHz for approximately 100 μs . In most of our experiments a pulse discriminator was set slightly above the

noise level to detect the start of the acoustic signal and to produce an easily handled, single pulse in near coincidence with this event. Extreme care was taken to measure one AE pulse per burst and to insure that the discriminator output was as near as possible in coincidence with the beginning of the AE burst. With the AC 1500 L transducer we estimate that the discriminator output pulse is $1.8 \pm 0.5 \mu\text{s}$ after the onset of the AE event, taking into account both the time required for the stress wave to reach the transducer crystal and amplifier rise-times.

C. Results

1. AE and Oxide Cracking

To determine the role of the anodized layer in the production of AE we tested several unanodized Al 1350 samples. With the exception of a small peak which occurs in the elastic portion of the stress strain curve (also observed with anodized samples), the AE bursts observed were negligible in number. The anodized samples, on the other hand, produced a total of 10,000 to 20,000 detectable AE bursts when strained to 10%. This led us to the hypothesis that the AE bursts are due to cracking of the oxide coating. Further supporting evidence was obtained by directly observing the initiation and incremental growth of cracks in the oxide in air under an optical microscope (100x) while simultaneously listening to the demodulated AE bursts over a loudspeaker. A significant number of the two events appeared to coincide. We are attempting to quantify these results by simultaneous video and audio recording.

In addition, the average length of both new cracks and the increments of crack growth was observed under the microscope to be about 0.1 mm. A measurement of total crack length in the oxidized area leads to an estimate of roughly 12,000 increments in crack growth during the experiment (10% strain).

This is consistent with the total AE counts we observe, again indicating that the oxide cracking is the source of the AE.

Finally, the characteristic acoustic emission curve (AE count rate vs strain) for samples strained in air differ strikingly from samples strained in vacuum. For samples strained in air the onset of AE and peak positions are shifted to a strain about 1% lower than in vacuum and the total AE is about 40% of the AE detected in vacuum. These differences are attributed to the changes in the mechanical properties of the oxide in air vs vacuum. (A prime suspect is H₂O vapor absorption.)^(2,17) For anodized samples strained in air, optical microscopy shows that the rate of crack growth as a function of strain, correlates very well with the AE characteristic curve. Again, this supports the hypothesis that the observed AE bursts result from oxide cracking.

2. Characteristic Emission Curves for Anodized Al 1350 Strained in Vacuum

The characteristic AE and EE curves taken simultaneously with two count rate meters are shown in Fig. 6 for a dense oxide on Al 1350. The close correlation between the two types of emission thus supports our early hypothesis that the EE is caused by cracking of the oxide layer.^(3,15)

Recording AE and EE simultaneously at a lower strain rate assured that the absolute rates of detected emission were determined accurately. This provided an accurate ratio of EE to AE as a function of strain. Typical AE, EE, and EE/AE curves are shown in Fig. 7. The ratio is near unity and indeed depends on strain. During the initial rise of the major peak (near 2% strain) the cracking of the oxide appears to be noticeably more "efficient" in producing electrons. Optical microscopy shows that these are the initial cracks formed in the oxide whereas the cracking occurring later is primarily crack extension. In the central portion of the emission curves the ratio is near unity and constant. Finally, the ratio climbs as the AE curve is seen to drop

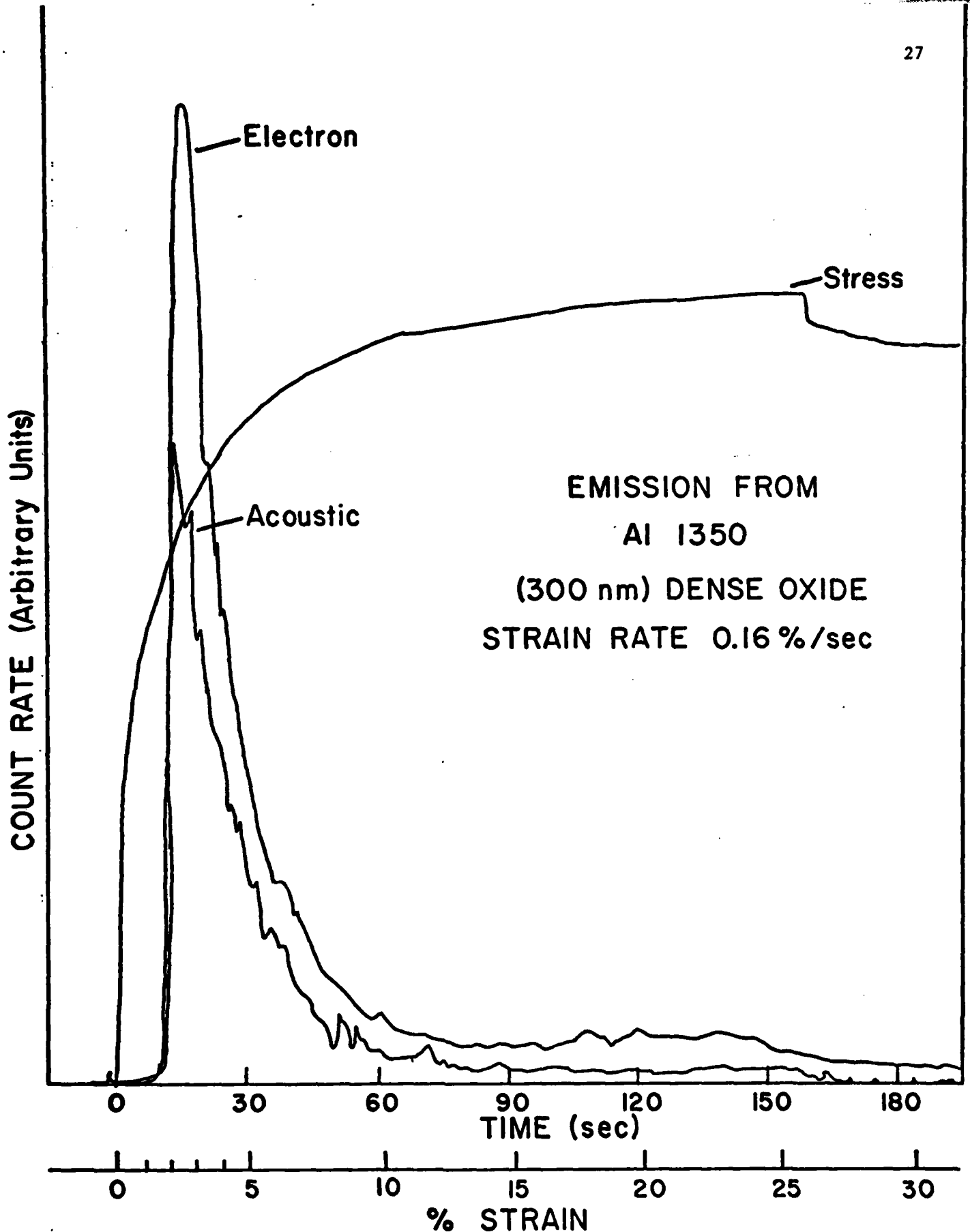


Fig. 6. Acoustic emission, exoelectron emission and stress, all versus strain or time, for a sample of anodized Al 1350.

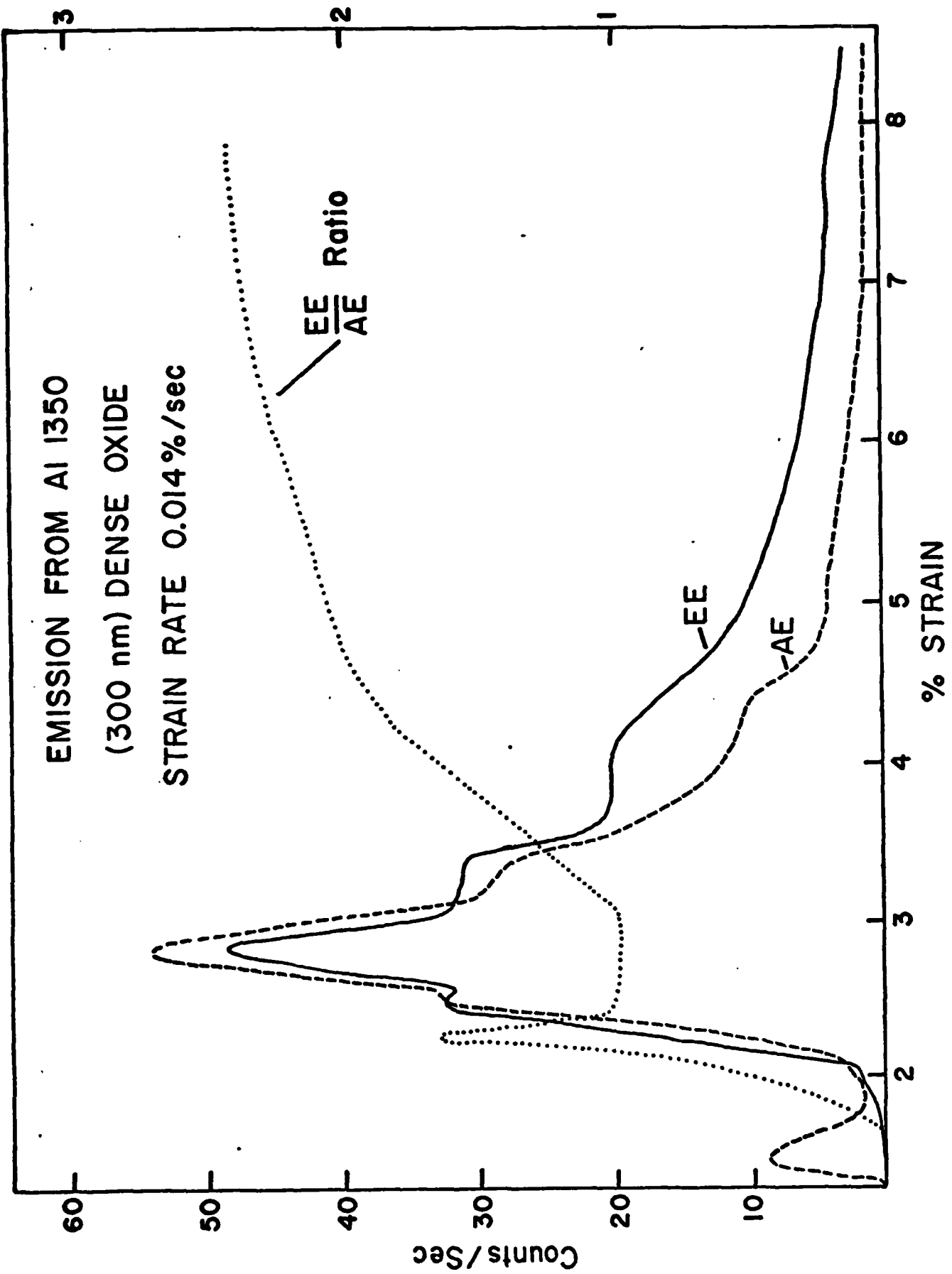


Fig. 7. EE and AE rates and their ratio (EE/AE) as a function of strain for a sample of anodized Al 1350.

off faster than the EE curve. We believe this increase is due to chemi-emission, as we will discuss shortly.

3. Correlation of AE and EE--Slow Time Scale

Another basic question is the time relation between AE and EE. If one pulls the sample very slowly, the bursts of AE and EE can be displayed as single events by means of suitable pulse shaping and the use of two synchronized strip chart recorders. A Two Graduate Student Coincidence Detector (TGSCD) was used to detect EE and AE events in and out of coincidence. We estimate our particular TGSCD could detect coincidences between the two types of bursts to within about 0.1 s. The results are as follows:

1. Near the peak of the emission, most of the electron bursts are in coincidence with AE bursts. Those EE bursts out of coincidence with AE bursts can for the most part be accounted for by background (2-3 counts per minute). This implies that EE occurs within roughly 0.1 s of the propagation of a crack in the oxide. (See Fig. 8a.)
2. Near the peak of emission, the majority of the AE bursts occur without an accompanying electron. However, the ratio of EE/AE in this region remains near unity, which implies that many electron bursts consist of more than one electron. We calculate an average of three electrons per burst. This is substantiated by display of the electron pulses on an oscilloscope. Usually single pulses are observed, but often two, three, or more occur within a few microseconds.
3. If the above "coincidence" experiment is performed after the elongation of the sample has been stopped, ^(see Fig. 8b) one finds that the

CORRELATION OF EE AND AE IN TIME

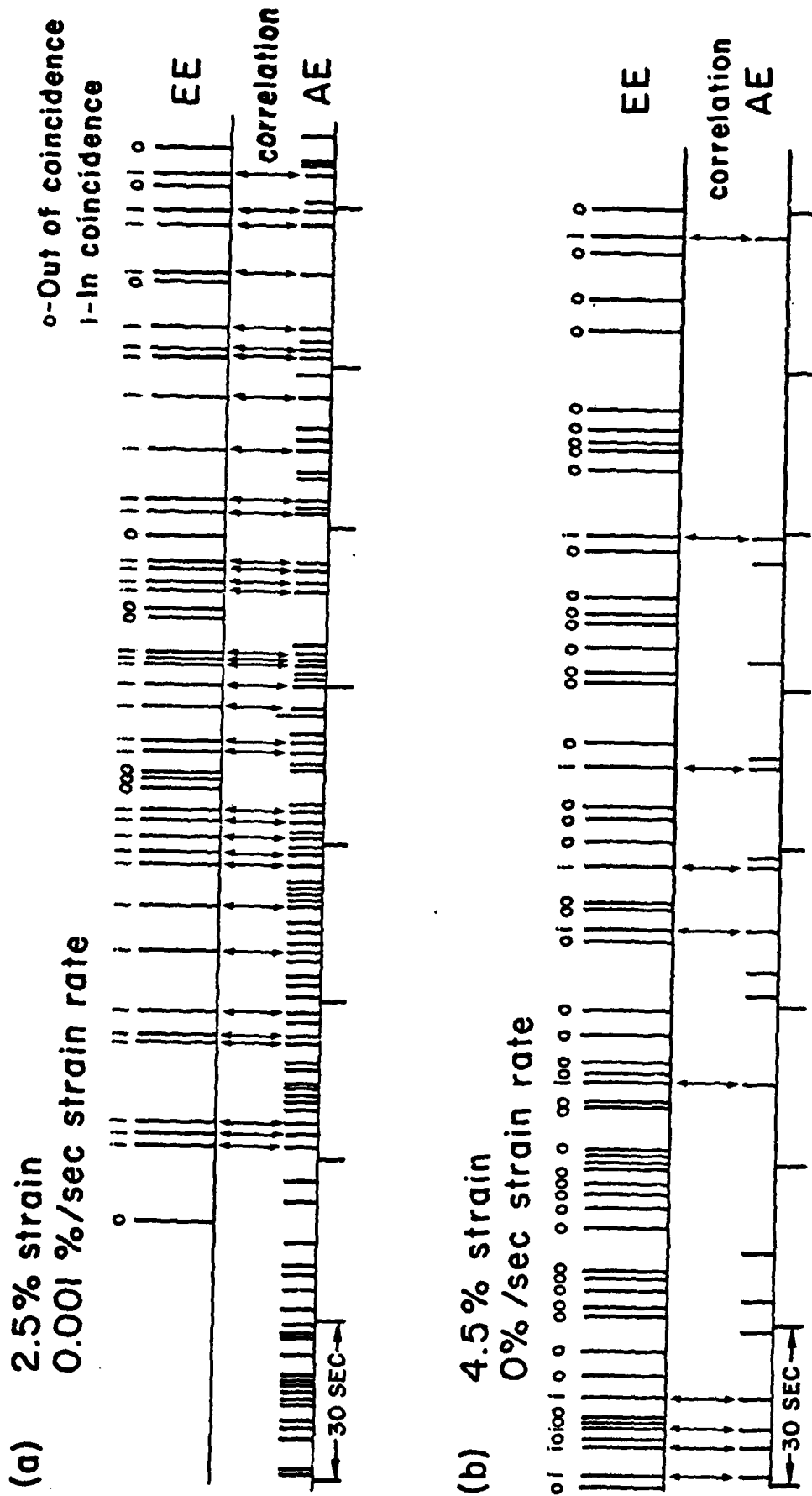


Fig. 8. Position in time of bursts of electrons (EE) and acoustic emission (AE) showing the correlation between them. a. During the peak of electron emission (very high correlation) and b. at larger strain and no sample extension.

AE drops quickly to zero, but a small very slowly decreasing EE component continues. It is this random component which we attribute to chemi-emission⁽¹⁸⁾ due to the reaction of gaseous species with the fresh Al surface exposed by cracking of the oxide. The source of the gas could be the oxide itself⁽¹⁵⁾ or it could be the 10^{-4} Pa background gas.

4. Time Correlation between AE and EE-- μ s Time Scale

A multichannel scaler with time-of-flight (TOF) capability was used to determine the distribution of electrons in time relative to an acoustic burst. Because the acoustic waves took a finite time to propagate from crack to transducer, it was necessary to delay the electron pulses in order to display their entire time distribution. Figure 9a shows the resulting distribution on a time-scale of 1 μ s channel. The $t = 0$ mark is uncertain to about $\pm 0.5 \mu$ s ($\pm 1/2$ channel). Oscilloscope traces of the AE bursts show that frequently the amplitude of the signals takes several cycles to reach a maximum. The structure seen on the left-hand side of the peak is due to triggering the TOF unit on an oscillation other than the first in the AE ringing burst. If one raises the discriminator level a few percent, the features before $t = 0$ grow considerably, becoming larger than the $t = 0$ peak. Figure 9b is another time distribution obtained at $1/4 \mu$ s/channel. The "spike" at $t = 0$ takes on a finite width and decay time. The time constants for the electron emission decay following the peak are about $3/4 \pm 1 \mu$ sec and a slower decay of $5 \pm 1 \mu$ sec. Any decay faster than $3/4 \mu$ sec would probably not be observable due to the finite rise-times and jitter in the pulse electronics. Thus the observed time distribution is consistent with a process or processes that decay in $\leq 3/4 \mu$ s and in $5 \pm 1 \mu$ s.

As mentioned earlier, some EE signals come in bursts of more than one electron. By triggering the TOF unit with the first electron in the burst, we

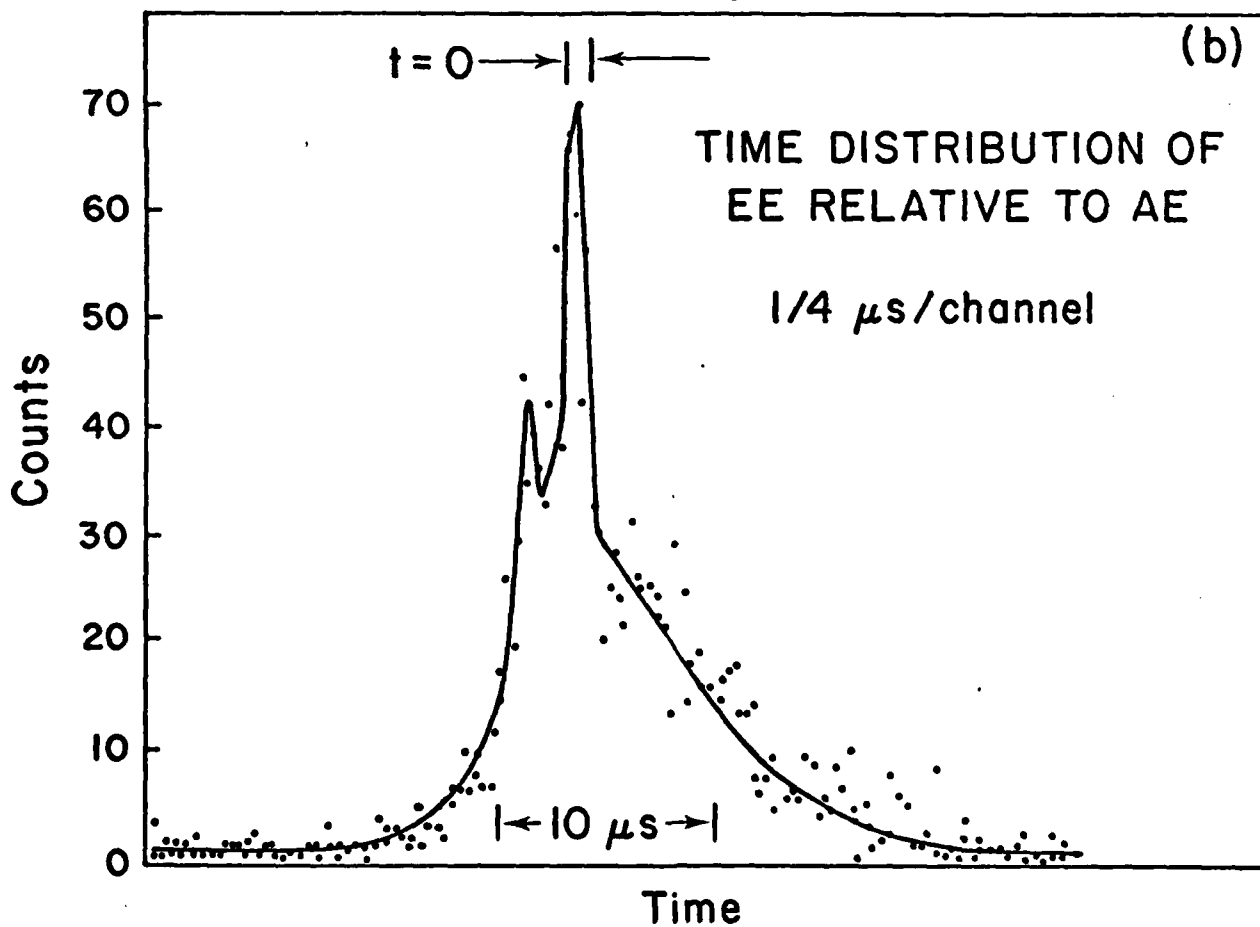
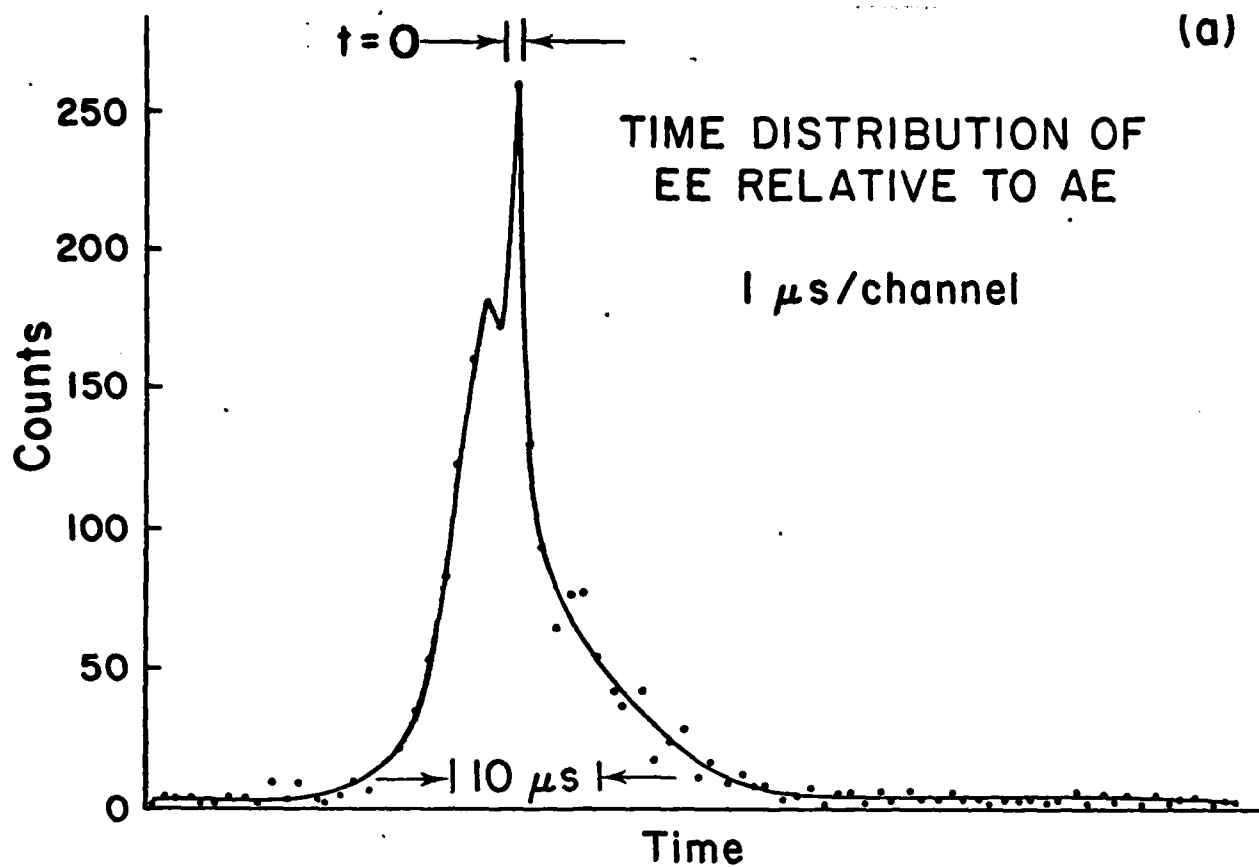


Fig. 9. a. Distribution of EE in time relative to AE at 1 $\mu\text{s}/\text{channel}$. The $t = 0$ point is shown to be uncertain by $\pm 0.5 \mu\text{s}$.
 b. Data similar to Fig. 9a taken at 1/4 $\mu\text{s}/\text{channel}$.

could obtain the time distribution of the remaining electrons in the burst (with the exception of those within 1 μ s of the first electron). We found an exponentially decaying function with a time constant of $4 \pm 1 \mu$ s. Thus, the slower decay observed in Fig. 9a and 9b could be due to the decay in the multiple electron bursts.

EE time distributions relative to AE taken at 8 μ s channel show decay components of even longer time constants; about 30 and 200 μ s.

D. Discussion

The AE bursts which we detect for these samples are clearly associated with the cracking of the anodic oxide coating and closely accompany actual propagation of the crack tip. The observed EE correlates strongly with the AE. This correlation is revealed on both a long time scale (Figs. 1 and 2) and a short time scale (Figs. 9a and 9b).

Within our uncertainty in the position of $t = 0$, the peak of the EE relative to AE occurs in coincidence. The decay from the peak ^{exhibits} \wedge a number of time constants _{and} suggests that a number of mechanisms may be involved. Also, we have established that the highest rate of electron emission occurs very near the onset of crack propagation. For brittle materials, cracks propagate at near the speed of sound, ⁽¹⁹⁾ implying that 0.1 mm long cracks grow in times on the order of 0.1 μ s. Thus, the electrons emitted in the narrow peak near $t = 0$ are leaving the sample in times less than a few tenths of a μ s following crack propagation and it is very likely they actually accompany crack propagation.

The slower 5 μ s decay, which involves a substantial fraction of the emission, occurs after the crack tip has come to rest. The exponential decay indicates a mechanism which relaxes relatively slowly when compared with most electronic processes. A highly localized thermal excitation (i.e., thermionic emission) as suggested by Arnott and Ramsey⁽⁹⁾ is not inconsistent with such a decay. Also, recent measurements on cracks propagated through glass and quartz by Weichert and Schönert⁽¹⁹⁾ show that temperatures on the order of 3000-4000 K were reached. Such temperatures could produce thermionic emission from the oxide. Another mechanism which is not inconsistent with our results is the electrified fissure model wherein crack propagation in the oxide produces charge separation across opposing crack faces. This charge separation produces strong electric fields which lead to field emission from the crack walls. The leakage of the charge to the substrate could account for the decay.

Clearly, our recent results provide strong evidence that tribostimulated exoemission accompanies and follows the propagation of cracks in the oxide film on the time scale of submicroseconds and microseconds. Hopefully, this new information will provide a basis for testing theoretical models of electron emission during and following crack propagation.

V. EMISSION OF Cl ATOMS FROM NaCl DURING

V_k -CENTER DECOMPOSITION

A. Introduction

In search of a clearer picture of mechanisms for the observed particle emission accompanying and following crack propagation, we decided to explore a simpler system where more is known about the intermediate states prior to thermal stimulation of the emission processes. It has been long known that electron and UV bombardment of alkali halides produces significant densities of near surface defects as long as the kinetic energies of the incident particles is sufficient to produce electron-hole pairs.⁽²⁰⁻²⁷⁾ Although this mode of defect production may not be available during fracture of an amorphous material such as an anodized oxide layer, there is very likely analogous defects produced. Following fracture the temperature of the material near the crack is certainly sufficient to cause a number of transformations (e.g. defect recombination) that could lead to emission. Thus to better understand some of these mechanisms we turned to a classic system, NaCl.

In NaCl and other alkali halides the formation of primary defects has been established to occur according to the following reactions:^(20,25,29)

- (1) energy absorption \rightarrow excitons (e-h pairs);
- (2) hole self-rapping $\rightarrow V_k$ -center;
- (3) trapping of an electron by a V_k -center \rightarrow F-H pair.

Step three has been shown to be very fast (several picoseconds) and highly competitive with two other possible channels of energy deposition to the lattice during electron trapping by a V_k -center, namely luminescence or heat generation.⁽²⁵⁾

While the formed F-center may be stable up to 500K in NaCl, the H-center (a Cl interstitial) moves quickly to the surface or recombines with

an F-center above 70K.^(30,31) In the absence of free electrons, V_k -centers⁽²³⁾ (Cl_2^- molecules, occupying two Cl lattice sites in the $\langle 110 \rangle$ direction are stable below 150K and decompose at about 165K, with an activation energy of 0.27 eV.⁽²⁰⁾ In the bulk, this process may be considered as thermal release of the self-trapped hole. Continued retrapping and release of holes is equivalent to V_k -center migration.

The emission of atomic halogen during electron bombardment or photon exposure (often referred to as sputtering⁽²⁰⁾) has frequently been explained as the result of a replacement collision sequence.^(20,26,27,32-35) V_k -centers, recombining with electrons, are believed to be able to impart sufficient kinetic energy to a neighbor Cl^- ion along a $\langle 110 \rangle$ direction to leave a vacancy (F-center) behind. Termination of the collision chain on the surface could result in halogen atom emission. The recent observation of strong atomic halogen emission in other directions (notably $\langle 211 \rangle$) suggests that such a sequence may consist of only one step.^(21,25) On the surface, an arriving or freshly formed V_k -center is assumed to simply decompose into a regular Cl^- ion bound to the lattice and a surplus Cl atom which can be emitted.^(20,21) Although the kinetic energy of the ejected Cl atom is very small,⁽⁷⁾ the emission is directional because the Cl_2^- molecule (V_k -center) breaks up along its bonding direction. Apparently it is not only oriented in a $\langle 110 \rangle$ direction but, on the surface, it may possibly be found also in $\langle 211 \rangle$ directions.⁽²¹⁾

Except for Brunsmann et al.⁽³⁶⁾ and Krylova,⁽³⁷⁾ no one has searched for particles other than electrons. On the other hand, a clear correlation, e.g. with the annealing temperature of the V_k -center and the appearance of a characteristic exoelectron emission peak at about 165K, has led Bichevin and Kaambre⁽³⁸⁾ to conclude that electrons are emitted in a process that involves the release of self-trapped holes. They further propose that these in turn

recombine with trapped electrons and, in an Auger-transition, impart energy to surface electron traps which eject electrons into the vacuum. It is certainly quite conceivable that analogous processes could occur following fracture of a material such as the anodized oxide layer.

In this work, we have investigated the emission of particles (electrons, neutrals, and ions) from NaCl during temperature programme' annealing of the surface layer, previously disturbed by e-beam sputtering at 100K. While we observed a number of emission phenomena, we were able to prove, for the first time, that V_k -center annealing can lead to atomic chlorine emission and, in addition, a metallic Na overlayer is formed during sputtering which desorbs from the surface as neutral atomic Na at about 400K.

B. Experimental Procedure

The NaCl crystals (1 mm x 36 mm², Harshaw Laser grade) were clamped to a 0.5 mm thick piece of tantalum that was cooled conductively to 100K and heated resistively. <100> surfaces of the samples were bombarded at 100K with 1.5 keV electrons (with a total dose of approximately 10^{15} e cm⁻²), using a defocussed beam from an Auger electron gun and subsequently heated at a linear rate of 0.5K sec⁻¹ while the particle emission was monitored as a function of sample temperature. This experimental procedure is known as thermally stimulated exoemission.

The experiments were carried out at 10^{-7} Pa (10^{-9} Torr) in a UHV system equipped with a quadrupole mass spectrometer and an Auger cylindrical mirror analyzer, a Channeltron electron multiplier for detection of charged particles and coils for magnetic discrimination (efficiency 98%) between low energy electrons and negative ions. Cl atom emission was distinguished from molecular emission by use of the mass 35 and mass 70 mass spectrometer signals. Cl₂ gas yielded a mass 35 to 70 ratio of 0.4 in our quadrupole mass spectrometer. The atomic Cl emission peak yielded no measurable mass 70 signal.

C. Results

The search for atomic Cl emission from NaCl surfaces after exposure to electrons at 100K initially produced negative results. Only the well-known electron emission peaks (prominent ones, depending somewhat on the heating rate, occur at about 165, 240, 300, and 500K⁽³⁸⁾ were observed during thermal stimulation, all of which are accompanied by a much weaker emission of negative chlorine ions (Fig. 10). The metallic Na overlayer, expected to be produced during sputtering,⁽²⁴⁾ was observed to desorb as neutral Na atoms via a first-order reaction peaking at 405K (Fig.10). Using the Redhead equation⁽³⁹⁾ we obtain an activation energy for desorption of approximately 1.01 eV, which is in good agreement with the heat of formation of gaseous⁽⁴⁰⁾ and ionic⁽²⁴⁾ Na from metallic sodium.

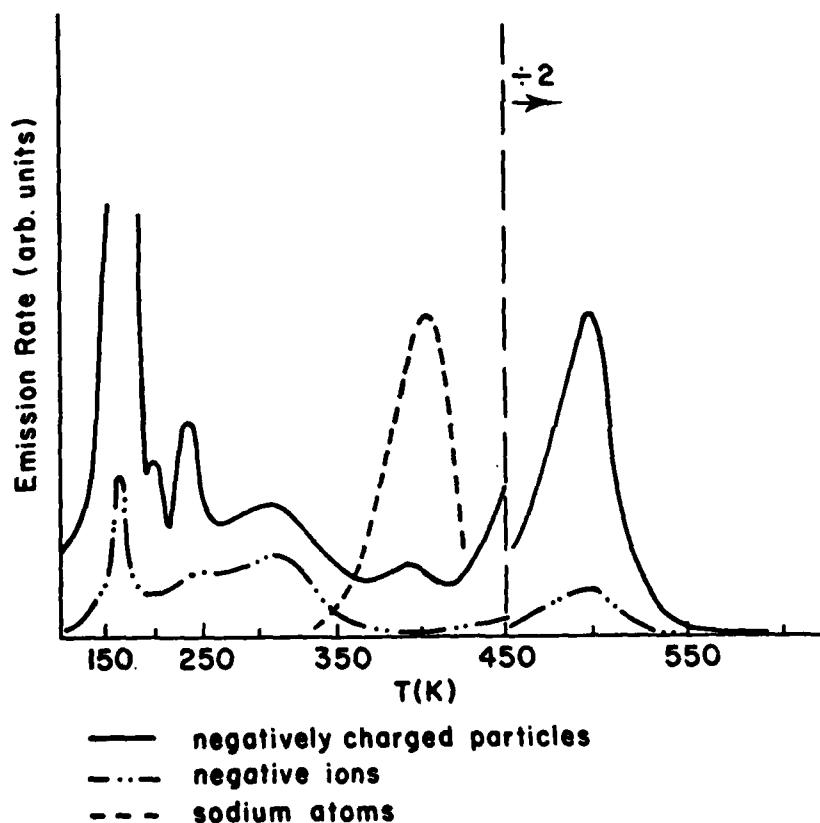


Fig. 10. Thermally stimulated emission of neutral and negatively charged particles following electron bombardment of NaCl at 100K (heating rate: 0.5K sec^{-1}).

The presence of the metallic Na layer at the temperatures of V_k -center migration has two immediate consequences.

(i) A V_k -center, arriving at this surface, reacts with Na to form NaCl and a Cl^- atom remains on a regular lattice site, thus, the Cl atom available from V_k decomposition is not emitted, and

(ii) the exothermic reaction between the Cl atom from the V_k -center and the metallic Na overlayer yields electron emission with a probability of at least 10^{-6} . This is deduced in the following manner: We neutralize the monolayer⁽²⁴⁾ of metallic Na, produced by e-beam sputtering, by exposing the surface to a saturation dose of Cl_2 gas and simultaneously monitor the total number of electrons chemi-emitted in the reaction $2Na + Cl_2 \rightarrow 2 NaCl$. The probability of electron emission that we obtain is in good agreement with the observations by Kasemo and Wallden⁽³⁹⁾ on the exposure of Na metal films to Cl_2 gas. Since the reaction between atomic chlorine and sodium is expected to be even more exothermic than between Cl_2 and sodium, we consider this value for the electron emission probability due to V_k decomposition to be a lower limit.

Consequently, the conversion of the metallic alkali layer to NaCl after electron bombardment and prior to V_k -center migration should prevent the formation of NaCl upon decomposition of V_k -centers on the surface and result in atomic Cl emission. That this is indeed so was shown after dosing the previously electron sputtered surface with Cl_2 at 100K. Subsequent heating and monitoring of the emitted particles resulted in the curve shown in Fig. 11.

For comparison the sodium desorption peak, obtained without a Cl_2 dose, has been added. Again, electron and negative ion emission is observed. Now, however, intense emission of Cl atoms occurs as well,⁽⁴²⁾ peaking at 165 and 300K (note that the detection efficiency for atoms is only about 10^{-8} of that for electrons and ions). Correlation with V_k -center annealing and

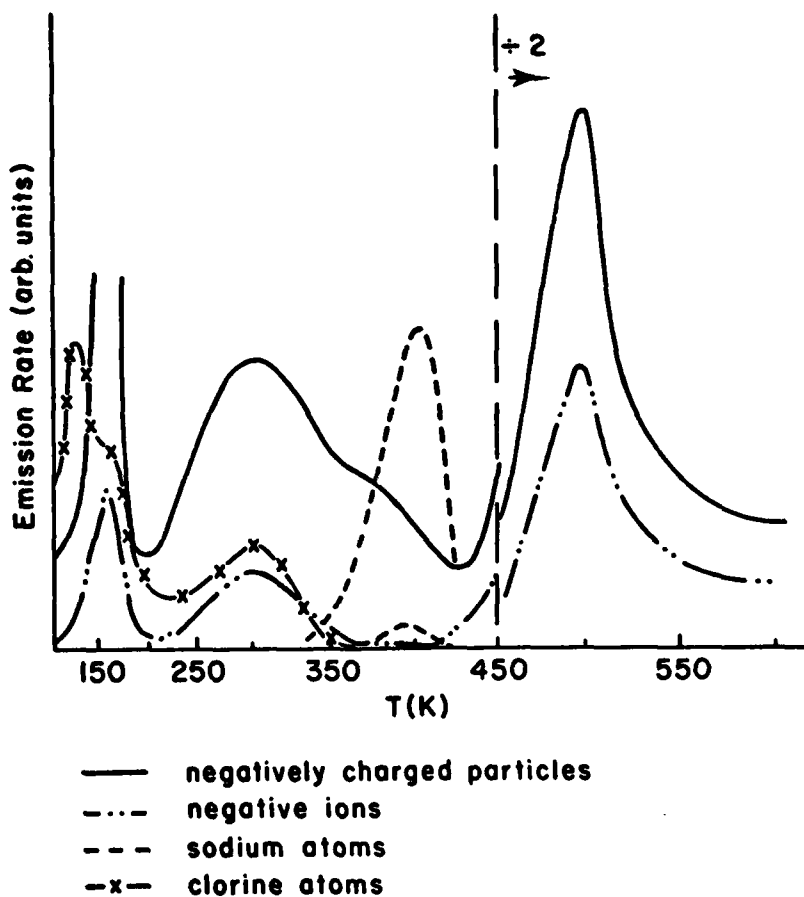


Fig. 11. Thermally stimulated particle emission from NaCl after electron bombardment and Cl_2 dose at 100K. A molecular chlorine desorption peak below 130K has been omitted and that for Na, obtained without Cl_2 dose, has been added (heating rate: 0.5K sec^{-1}). Mass 35 signal below 130K is due to conversion of Cl_2 (from Cl_2 desorption) to Cl^+ in the ionizer of the mass spectrometer.

exoelectron emission results⁽¹⁹⁾ established that the first of these peaks is due to V_k -center decomposition on the surface, thus providing direct evidence that it occurs according to $V_k + \text{Cl}^- (\text{lattice}) + \text{Cl} (\text{emitted})$. Measurements of the activation energy (0.29 eV obtained by applying the initial rise method⁽⁴³⁾ to the 165K electron peak) confirmed this assignment.⁽²⁰⁾ The nature of the second Cl emission peak is not clear at this time. It occurs in a temperature region in which F' and α -centers are known to combine, forming M-centers,⁽²³⁾ however, it is not obvious why this reaction should result in the ejection of

Cl atoms. The mechanism responsible for the weak emission of negative chlorine ions (Fig. 10) is also not understood at this point. Measurements of the steady-state Auger spectra during sample heating at the same rate of 0.5K sec^{-1} revealed distinct drops of the 181 eV Cl signal exactly in the temperature regions where the 240 and 300K ion peaks are observed. In addition, the first derivative of the Cl-Auger signal with respect to temperature reproduces the shape of these ion peaks in Fig. 10. This observation is in sharp contrast to a constant Cl-Auger signal during V_k -center annealing, where the effective Cl-coverage of the surface is not changed because migrating V_k -centers decompose to form NaCl in the presence of the metallic Na overlayer. We therefore feel that the appearance of the 240 and 300K ion peaks (and the 300K Cl atom peaks we well) is not due to migration of a center that carries Cl atoms to the surface but must instead be explained as some form of Cl defect formation in the surface layer.

The emission of electrons during V_k -center annealing after e-beam sputtering and after converting the metallic Na overlayer to NaCl was observed to be somewhat weaker as compared to the case when the surface was not dosed with Cl_2 . Since the chemical reaction between Cl and Na is now not possible; a different mechanism must be responsible for the 165K exoelectron emission peak. The following process is likely: the majority of V_k -centers arriving at the surface result in atomic Cl emission, detected with an efficiency of around 10^{-8} . Those which migrate toward a surface F' -center anneal according to the reaction $V_k + F' \rightarrow 2\text{Cl}^-(\text{lattice}) + e$. The electron is emitted and detected with an efficiency of close to unity, thus accounting for the relatively strong exoemission peak.

D. Conclusion

We have demonstrated that electron bombardment of NaCl below 400K produces an alkali-rich surface which prevents the observation of expected Cl emission during V_k -center decomposition. Conversion of this metallic layer to NaCl by Cl_2 exposure previous to V_k -center annealing permits one to directly observe atomic halogen ejection. The first order neutral Na desorption at 400K supports the idea of an overlayer of metallic Na.

Although this idealized system is quite different from the anodized oxide coating, there is a good possibility that the electron, ion, photon, and neutral emission we observe during film fracture are due to analogous processes. The propagation of a crack in a brittle material is an extremely energetic, rapid, and catastrophic event which can produce a multitude of near surface defects and filled electron traps at the surface. These can be converted to free electrons either thermally or via Auger-transitions driven by energy released from defect decomposition/recombination. Now that we are obtaining time dependent data on the emission relative to crack propagation, it might be possible to better identify the processes involved in the emission phenomena.

Furthermore, we make the observation that the observed neutral emission from anodized aluminum could have an origin similar to the Cl and/or Na emission in NaCl.

VI. CHEMILUMINESCENCE DURING H_3PO_4 ANODIZATION OF BARE Al 2024

When oxygen reacts with a clean metal surface two forms of particle emission have sometimes been observed: electrons and photons. The first is called chemi-emission and the second is called chemiluminescence. Exposure of Al to O_2 has yielded both chemi-emission⁽⁴⁴⁾ and chemiluminescence.⁽⁴⁵⁾ The observed luminescence seems to be in the visible spectrum and has a probability of around 10^{-5} photons per O_2 molecule reacting.

We hypothesized that such luminescence might be detectable from an aluminum sample during anodization in a H_3PO_4 solution under conditions like those used in the preparation of aluminum for epoxy bonding. Thus we performed a preliminary experiment using a photomultiplier (PM) tube sensitive to visible light only. The PM used was rather noisy but proved adequate. For this experiment at 1 kV, the dark current was 5×10^{-9} amps. Normally this PM would be run at much higher voltage 2.5 kV and therefore higher gain. A Keithley Electrometer was used to measure the PM output. The PM was pointed at an Al 2024 bare sample of about 4 cm^2 area (10 cm away from the PM tube) in a 1000 ml beaker containing a 10% H_3PO_4 solution. The cathode was also aluminum.

There was no difficulty in detecting photons which accompanied anodization. In fact, initially at 10 volts forming voltage, the detector saturated. The photon emission vs. time was a complicated function which depended on how long the sample stayed in the solution prior to turning on the voltage and on the current. The intensity was also strongly dependent on the applied voltage, being roughly proportional. The power supply used would not go below 3.5 volts, but at this voltage, substantial photon fluxes were still detected.

A sample of Al 1350, a relatively pure Al alloy, was also tried. It was also a good photon emitter. The intensity vs. time was completely different from the Al 2024 sample.

A literature search showed that a wide number of effects such as the above have been observed (see e.g. Ref. 46). However, we have not as yet found a study of luminescence during H_3PO_4 anodization.

Such emission could provide a very easy way to monitor anodization in a commercial situation. There appears to be sufficient intensity that spectroscopy could be performed which might allow the usefulness of a monitoring technique to be greatly expanded. If time permits we will pursue this effect further.

VII. PUBLICATIONS AND PRESENTATIONS

A. Publications

Characteristic Emission of Negatively Charged Particles During Tensile Deformation of Oxide-Covered Aluminum Alloys, J. T. Dickinson, P. Bräunlich, L. Larson, and A. Marceau, Applications of Surf. Sci. 1, 515 (1979).

The Emission of Neutral Particles from Anodized Aluminum Surfaces During Tensile Deformation, L. A. Larson, J. T. Dickinson, P. Bräunlich, D. Snyder, J. Vac. Sci. Technol. 16, 590 (1979).

Characterization of Anodic Oxide Coatings on Aluminum by Tribostimulated Exoemission, D. L. Doering, T. Oda, J. T. Dickinson, and P. Bräunlich, Applications of Surf. Sci. 3, 196 (1979).

Emission of Cl Atoms from NaCl during V_k-Center Decomposition, L. A. Larson, T. Oda, P. Bräunlich, and J. T. Dickinson, Solid State Communications 32, 347 (1979).

Tribostimulated Emission of Electrons and Neutral Particles from Anodized Aluminum, J. T. Dickinson and P. Bräunlich, Proceedings of the ARPA/AFOSR Conference on NDA, La Jolla, CA (1979), to be published.

Acoustic Emission and Electron Emission During Deformation of Anodized Aluminum, J. T. Dickinson, D. B. Snyder, and E. E. Donaldson, J.V.S.T. (accepted for publication).

Experiments on Exoemission During Oxide Coating Fracture, J. T. Dickinson and P. Bräunlich, Proceedings of the International Symposium on Exoemission and Applications, Rostock, E. Germany (Oct. 1979), to be published.

Thermostimulated Processes at Surfaces of Solids, P. Bräunlich and J. T. Dickinson, Proceedings of the VI International Symposium on Exoemission and Applications, Rostock, E. Germany (October 1979), to be published.

B. Presentations

"Tribo-Stimulated Exoemission," Invited Talk, Battelle Northwest (August, 1977).

"Characteristic Emission of Negatively Charged Particles During Tensile Deformation of Oxide-Covered Aluminum Alloys," ASM-AIME Conference, Chicago (October, 1977).

First Author of Paper "The Adsorptive/Reactive Interactions of H₂CO on a Ni(110) Surface," Third International Conference on Solid Surfaces, Vienna (September, 1977).

"Chemisorption of CO on Supported Pd Particles," AVS Conference, October, 1977.

"The Emission of Neutral Particles from Anodized Aluminum Surfaces During Tensile Deformation," AVS Conference, November, 1978.

"On the Mechanism of Tribostimulated Exoemission from Anodized Al Surfaces," AVS Conference (New York, 1979).

"Tribostimulated Emission of Electrons and Neutral Particles from Anodized Aluminum," ARPA/AFOSR Conference on NDA, La Jolla, CA (July, 1979).

"Exoemission During Oxide Coating Fracture," Invited Talk, Vith Int. Conf. on Exoemission and Applications, Rostock, E. German (1979).

"Thermostimulated Processes at Surfaces of Solids," Invited Talk, VI International Symposium on Exoemission and Applications, Rostock, E. Germany (1979).

VIII. REFERENCES

1. J. T. Dickinson, P. F. Braunlich, L. A. Larson, and A. Marceau, *Appl. of Surf. Sci.* 1, 515 (1979).
2. D. L. Doering, T. Oda, J. T. Dickinson, and P. Braunlich, *Appl. of Surf. Sci.* 3, 196 (1979).
3. B. Z. Rosenblum, P. F. Braunlich, and L. Himmel, *J. Appl. Phys.* 48, 5262 (1977).
4. R. G. Liptai and R. G. Tatro, "Proceedings of the Fourth Annual Symposium on Non-destructive Testing of Aircraft and Missile Components," 284-346, Southwest Research Institute, San Antonio, Texas, 1963.
5. R. G. Liptai, "An Investigation of the Acoustic Emission Phenomenon," Ph.D. Thesis, Michigan State University, East Lansing, Michigan, 1963.
6. H. L. Dunegan and D. A. Tatro, "Acoustic Emission Effects During Mechanical Deformation," 243-312, *Techniques of Metals Research*, Vol. 4, Interscience Publishers, John Wiley and Sons (New York, 1971).
7. B. Z. Rosenblum, J. P. Carrico, P. F. Braunlich, and L. Himmel, *J. Phys.* 10, 1056 (1977).
8. L. R. Danielson, M. J. Dresser, E. E. Donaldson, and J. T. Dickinson, *Surf. Sci.* 71, 599 (1978).
9. D. R. Arnott and J. A. Ramsey, *Surf. Sci.* 28, 1 (1971).
10. J. W. Diggle, T. C. Downie, and C. W. Goulding, *Chem. Rev.* 69, 365 (1969).
11. J. E. Lewis and R. C. Plumb, *J. Electrochem. Soc.* 105, 496 (1958).
12. R. B. Mason, *J. Electrochem. Soc.* 102, 671 (1955).
13. R. E. Herfort, "Fundamental Investigation of Anodic Oxide Films on Aluminum Alloys as a Surface Preparation for Adhesive Bonding," U.S. Air Force Technical Report AFML-TR-76-142.
14. C. S. Taylor, C. M. Tucker, and J. D. Edwards, *Trans. Electrochem. Soc.* 88, 325 (1945).
15. L. A. Larson, J. T. Dickinson, P. F. Braunlich, and D. B. Snyder, *J. Vac. Sci. Technol.* 16, 590 (1979).
16. E. A. Kurz, American Laboratory, March 1979, p. 67.
17. J. C. Grosskreutz, *Surf. Sci.* 8, 173 (1967).
18. N. K. Saadeh and J. Olmsted III, *J. Phys. Chem.* 79, 1325 (1975).
19. R. Weichert and K. Schonert, *J. Mech. Phys. Solids* 26, 151 (1978).

20. P. D. Townsend, R. Browning, D. J. Garland, J. C. Kelly, A. Majhoobi, A. J. Michael, and M. Saidoh, *Rad. Eff.* 30, 55 (1976).
21. A. Schmid, P. Braunlich, and P. Rol, *Phys. Rev. Lett.* 35, 1382 (1975).
22. N. Itoh, *Cryst. Latt. Defects* 3, 115 (1972).
23. E. Sonder and W. Sibley, *Point Defects in Solids* (Edited by J. H. Crawford and L. M. Slifkin), Vol. 1, Plenum Press, New York and London (1972).
24. Y. Al Jammal and P. D. Townsend, *J. Phys.* C6, 955 (1973).
25. M. N. Kabler and R. T. Williams, *Phys. Rev.* B18, 194 (1978).
26. H. Overeijnder, *Rad. Eff.* 36, 63 (1978).
27. N. Itoh, *Nucl. Instr. Meth.* 132, 201 (1976).
28. A. W. Czanderna (ed.), *Methods of Surface Analysis*, Elsevier, New York (1975).
29. R. T. Williams, *Semicond. and Insulators* 3, 251 (1978).
30. N. Itoh, *J. Phys. Colloq.* 37, C7 (1976).
31. Y. Farge, *J. Phys. Colloq.* 34, C9 (1973).
32. D. Pooley, *Proc. Phys. Soc.* 87, 245 (1966).
33. H. Hersh, *Phys. Rev.* 148, 928 (1966).
34. R. Smoluchowski, *Phys. Rev. Lett.* 35, 1385 (1975).
35. P. D. Townsend, *Phys. Rev. Lett.* 36, 827 (1976).
36. U. Brunsmann and A. Scharmann, *Phys. Status Solidi (a)* 43, 519 (1977).
37. I. V. Krylova, *Russ. Chem. Rev.* 45, 1101 (1976).
38. V. Bichevin and H. Kaambre, *Phys. Status Solidi (a)* 4, K235 (1971).
39. P. A. Redhead, *Vacuum* 12, 203 (1962).
40. 1.02 eV; *Handbook of Chem. and Phys.* 54th edition, p. D-58. CRC Press, Cleveland (1973-74).
41. B. Kasemo and L. Wallden, *Surf. Sci.* 53, 393 (1971).
42. Atomic Cl emission, measured below 130K, is readily identified as the result of Cl₂ desorption after Cl₂ dosing. A fraction (approx. 0.4) of the mass spectrometer and thus monitored as atomic Cl.

43. K. Becker, *CRC Critical Reviews in Solid State Sciences* 3, 39 (1972).
44. J. A. Ramsey, *Surf. Sci.* 8, 313 (1967).
45. J. Harris, B. Kasemo, and E. Tornqvist, *Chem. Phys. Lett.* 52, 538 (1977).
46. S. Ikonopisov, *Electrochimica Acta* 20, 783 (1975).